Available online at www.sciencedirect.com

ScienceDirect

Palaeoworld 33 (2024) 229–240

Palaeoworld

www.elsevier.com/locate/palwor

Taxonomy and phylogeny of the smallest Miocene rhinocerotid *Parvorhinus* n. gen. (Mammalia, Rhinocerotidae)

Luca Pandolfi [a,*], Roberta Martino [b,c]

[a] *Department of Science, University of Basilicata, viale dell'Ateneo Lucano 10, 85100 Potenza, Italy*
[b] *Department of Earth Sciences, GeoBioTec, School of Science and Technology, FCT-NOVA, Universidade NOVA de Lisboa, Campus de Caparica, 2829-516 Caparica, Portugal*
[c] *Museu da Lourinhã, R. João Luís Moura, 95, 2530-158, Lourinhã, Portugal*

Received 28 October 2022; received in revised form 1 December 2022; accepted 11 January 2023
Available online 20 January 2023

Abstract

Middle Miocene Rhinocerotini are particularly important to understand the origin and evolution of latest Miocene and then Plio-Pleistocene taxa. However, little is known about some early divergent Rhinocerotina such as '*Dicerorhinus*' *steinheimensis*. A sample of a small-sized rhinocerotid from the Middle Miocene (Mammal Neogene Zone 6) locality of Devínska Nová Ves (Bratislava, Slovakia) is here described for the first time. The specimens consist of maxillae, fragment of mandibles and postcranial remains. The described specimens clearly differ from Middle Miocene representatives of elasmotheres, aceratheres and brachypotheres, but closely resemble the poorly known rhinocerotid '*Dicerorhinus*' *steinheimensis*. A cladistic analysis shows that this taxon is related with the early divergent Rhinocerotina, such as *Lartetotherium sansaniense* and *Gaindatherium browni*, and it is distantly related with both *Rhinoceros* and *Dicerorhinus*. Considering the position and the peculiar morphological and morphometric features, such as smaller size with respect to other Rhinocerotini species, posterior border of the symphysis in front of p2, crochet always present on P2-P4, P1 always absent, protoloph interrupted on P2, lingual cingulum absent on M1-M2, posterior part of the ectoloph concave on M1-M2, '*Dicerorhinus*' *steinheimensis* is here included in the new genus *Parvorhinus*.

Keywords: Middle Miocene; Rhinocerotina; *Parvorhinus* n. gen.; phylogeny; morphology

1. Introduction

Miocene European Rhinocerotidae has been a subject of a number of investigations during the past decades (Guérin, 1982; Heissig, 1999; Antoine et al., 2003; Jame et al., 2019; Becker and Tissier, 2020; Pandolfi et al., 2021a), which has increased our knowledge about their phylogeny, systematic and distribution. However, the origin and evolution of early representatives of Rhinocerotina, the group that includes the extant species and their fossil relatives, remain poorly investigated and highly debated. The main reason is the poor fossil record of some Middle Miocene representatives of this group such as '*Dicerorhinus*' *steinheimensis*. Nothing has been recently published or reported about this small-sized rhinocerotid, described during the first half of the 18th century as *Rhinoceros steinheimensis* Jaeger, 1839. This rare species is recorded in a few central European localities between the Mammal Neogene Zone (MN) 6 and 9 and it is at present documented only by isolated teeth, an extremely worn upper tooth serie and an incomplete lower tooth serie (Guérin, 1980, figs. 8D, 9D). No cranial or postcranial remains have been previously described (Jaeger, 1839;

* Corresponding author.
E-mail address: luca.pandolfi@unibas.it (L. Pandolfi).

https://doi.org/10.1016/j.palwor.2023.01.009

Guérin, 1980; Heissig, 1999), making this species problematic from both taxonomic and phylogenetic point of views.

Several cranial and postcranial remains, collected from the Middle Miocene (MN 6) locality of Devínska Nová Ves (Bratislava, Slovakia) (Zapfe, 1958, 1979; Sabol et al., 2021) and housed at Naturhistorisches Museum of Wien, are here described and compared, and referred to the Jaeger' species. The specimens here described are from the same level, have similar numeration and probably belong to the same individual. Accordingly, taxonomic and phylogenetic implications for early divergent Rhinocerotina are briefly discussed.

The fossil assemblage of Devínska Nová Ves–Štoker avská vápenka site (Fig. 1) was described for the first time by Zapfe (1949). This locality is particularly relevant because it testifies a gradual transition from terrestrial to marine conditions during the Badenian (Sabol et el., 2021 and references therein). The Devínska Nová Ves–Štoker avská vápenka faunal assemblage is particularly rich and includes primate such as *Pliopithecus vindobonensis*, rodents (e.g., *Democricetodon vindobonensis*, *Neocometes brunonis* and *Anomalomys gaudryi*), carnivores (e.g., *Pseudocyon steinheimensis* and *Ursavus brevirhinus*), artiodactyls (e.g., *Dorcatherium vindobonens* and *Palaeomeryx magnus*), and perissodactyls (e.g., *Anisodon grande*). For a more complete list see Sabol et al. (2021). The faunal composition unearthed and described from Devínska Nová Ves–Štokeravská vápenka unequivocally supports its assignment to unit MN6 (Sabol et al., 2021 and references therein).

2. Material and methods

The complete list of the studied specimens is reported as Supplementary data 1 along with the measurements (in mm) of each specimen. The material was directly compared with the rhinocerotid material collected from different Miocene localities of Europe as well as on the specimens published in several contributions. Some key-differences between the studied material and the considered Miocene

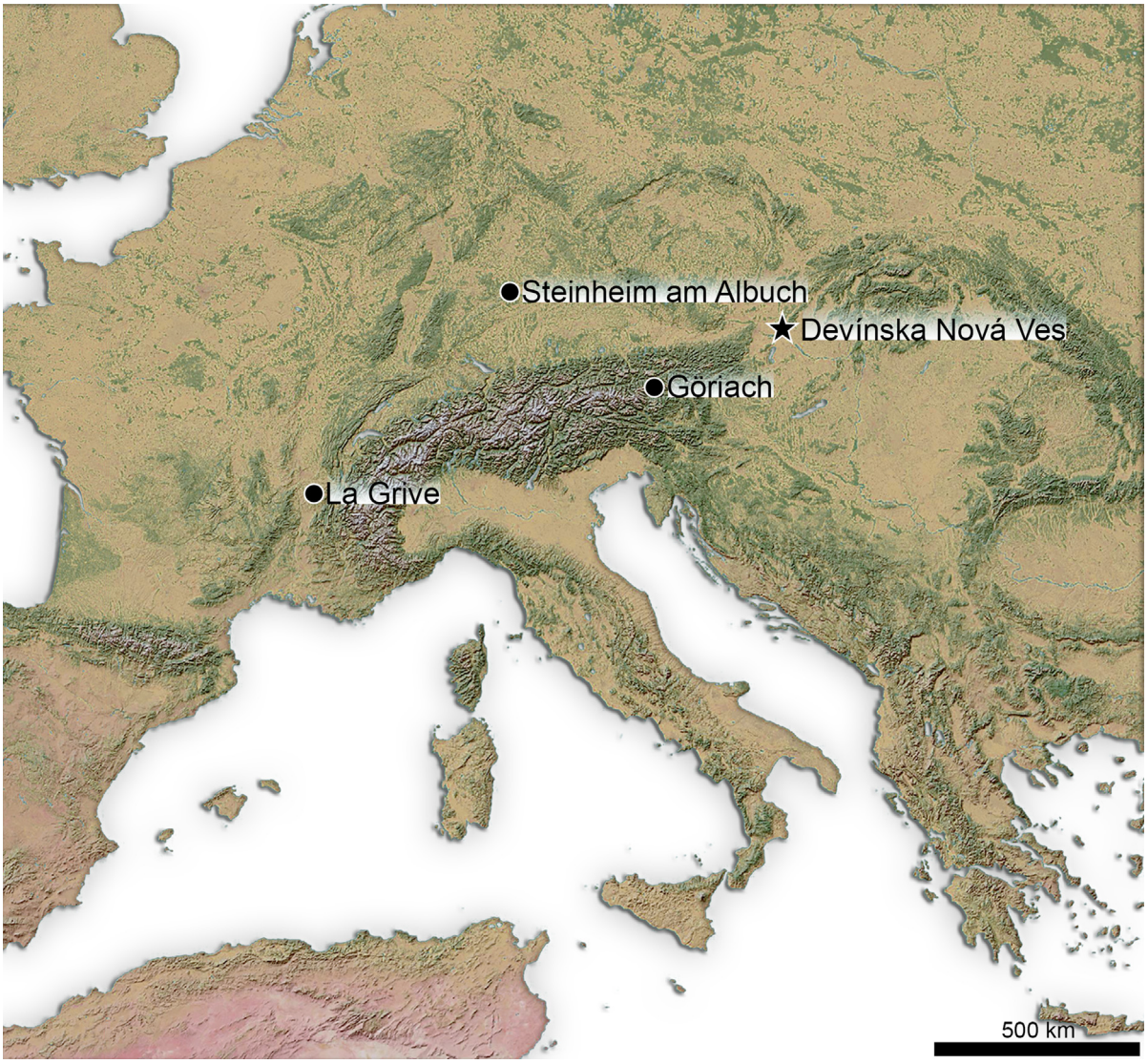

Fig. 1. Location map of the fossil locality of Devínska Nová Ves and other localities with *Parvorhinus steinheimensis* mentioned in the discussion.

taxa are listed in the text, but other differences can be detected in the Data Matrix (Supplementary data 2). The anatomical terminology follows that of Antoine (2002); the morphometric methodology follows Guérin (1980). A cladistic analysis was performed to infer the phylogenetic relationships of the rhinocerotid from Devínska Nová Ves; 284 characters yet described in literature (Boada-Saña, 2008; Deng et al., 2011; Pandolfi et al., 2021b; Uzunidis et al., 2022) were considered in this work (Supplementary data 3). All characters are equally weighted, 6 characters are unordered (68, 89, 97, 131, 179, and 265), 277 characters are ordered. The analysis was performed in PAUP 4.0β10 (Swofford, 2001), Heuristic search, TBR and 1000 replications with additional random sequence, gaps treated as missing. Thirty-one taxa, representatives of the main Eurasian clades were included in this analysis, four taxa are selected as outgroup: *Tapirus terrestris*, *Trigonias osborni*, *Hyrachyus eximius*, *Ronzotherium filholi*. The species *Rhinoceros steinheimensis* has been codified considering the studied material from Devínska Nová Ves, and the comparative material from the Middle Miocene localities of Steinheim, La Grive and Göriach, including juvenile specimens described by Toula (1884) and housed at NHMW (470/1963).

Institutional abbreviations: **MfN**, Museum für Naturkunde, Berlin, Germany; **MNCN**, Museo National de Ciencias Naturales, Madrid, Spain; **NHMUK**, Natural History Museum, London, England; **NHMW**, Naturhistorisches Museum, Wien, Austria; **NMB**, Naturhistorisches Museum, Basel, Switzerland; **SMNS**, Staatliches Museum für Naturkunde, Stuttgart, Germany.

Terminology: Anatomical abbreviations are as follows: **DP/dp** = upper/lower deciduous; **dx** = right; **P/p** = upper/lower premolar; **M/m** = upper/lower molar; **I/i** = upper/lower incisor; **MC** = metacarpal; **MT** = metatarsal; **sx** = left.

3. Systematic paleontology

Order Perissodactyla Owen, 1848
Family Rhinoceratidae Gray, 1821
Subfamily Rhinocerotinae Gray, 1821
Tribe Rhinocerotini Gray, 1821

Parvorhinus n. gen.
(Figs. 2–6)

Etymology: From the Latin "parvus", small, and "rhinus", nose.
Referred species: *Parvorhinus steinheimensis* (Jaeger, 1839).
Diagnosis: Same as for the species.
Distribution: Late early to early late Miocene (MN3-MN9) of Europe.

Parvorhinus steinheimensis n. comb.
(Figs. 2–6)

Lectotype: Isolated teeth figured by Jaeger (1839, pl. 1, and pl. 2, figs. 19, 20) and housed at SMNS.
Type locality and horizon: Steinheim am Albuch, Baden-Württemberg, Germany, Middle Miocene, MN7.
Emended diagnosis: *Parvorhinus steinheimensis* can be diagnosed by twenty three unambiguous autapomorphies: (1) subtriangular foramen magnum; (2) absence of the median ridge on the occipital condyles; (3) presence of the median truncation on the occipital condyles; (4) posterior border of the symphysis in front of p2; (5) lingual groove absent on the corpus mandibulae; (5) crochet always present on P2-P4; (6) P1 always absent; (7) protoloph interrupted on P2; (8) lingual cingulum absent on M1-M2; (9) posterior part of the ectoloph concave on M1-M2; (10) metaloph continuous on M1; (11) external groove reaching the neck on the lower cheek teeth; (12) angular trigonid on the lower cheek teeth; (13) dp1/p1 absent; (14) vertical external rugosities present on dp2-dp3; (15) posterior supraglenoid tubercle present on the scapula; (16) M-shaped anterior border of the proximal articulation on the radius; (17) posterior expansion of the scaphoid facet low on the radius; (18) anterior height taller that the posterior one on the scaphoid; (19) trapezium-facet usually present on MCII; (20) flat insertion of the muscle extensor carpalis on the metacarpals; (21) tibia-fibula in contact; (22) ratio between antero-posterior diameter and maximal height on the astragalus less than 0.65; (23) sinuous caudal border of the trochlea in the astragalus.

4. Description

4.1. Skull

The skull is represented by the palatine area with both maxillae and a portion of the basicranium (Fig. 2A, B). A few characters of the skull can be detected: the foramen infraorbitalis is located above the premolar-row, and the anterior border of the orbit lies above P4-M1. The processus lacrymalis is present and the base of the processus zygomaticus maxillary is high. In lateral view, the externa auditory pseudomeatus is ventrally opened. In basal view, the processus postglenoidalis has a concave cross section, and the sagittal crest on the basilar process is absent. The processi post-tympanicus and paraoccipitalis are distant and well-developed. The foramen magnum is subtriangular, the median ridge on the condyle is absent.

4.2. Upper teeth

The upper cheek teeth include P2, P3, P4, M1, M2, and M3 (Fig. 2C–E). The lingual border of the upper cheek tooth series is slightly concave, and the tooth crowns are relatively low with wrinkled enamel. Labial and lingual cingula are absent on the teeth, whilst a mesial cingulum occurs on P3-M3. On the premolars, paracone and metacone folds are prominent, and parastyle and metastyle

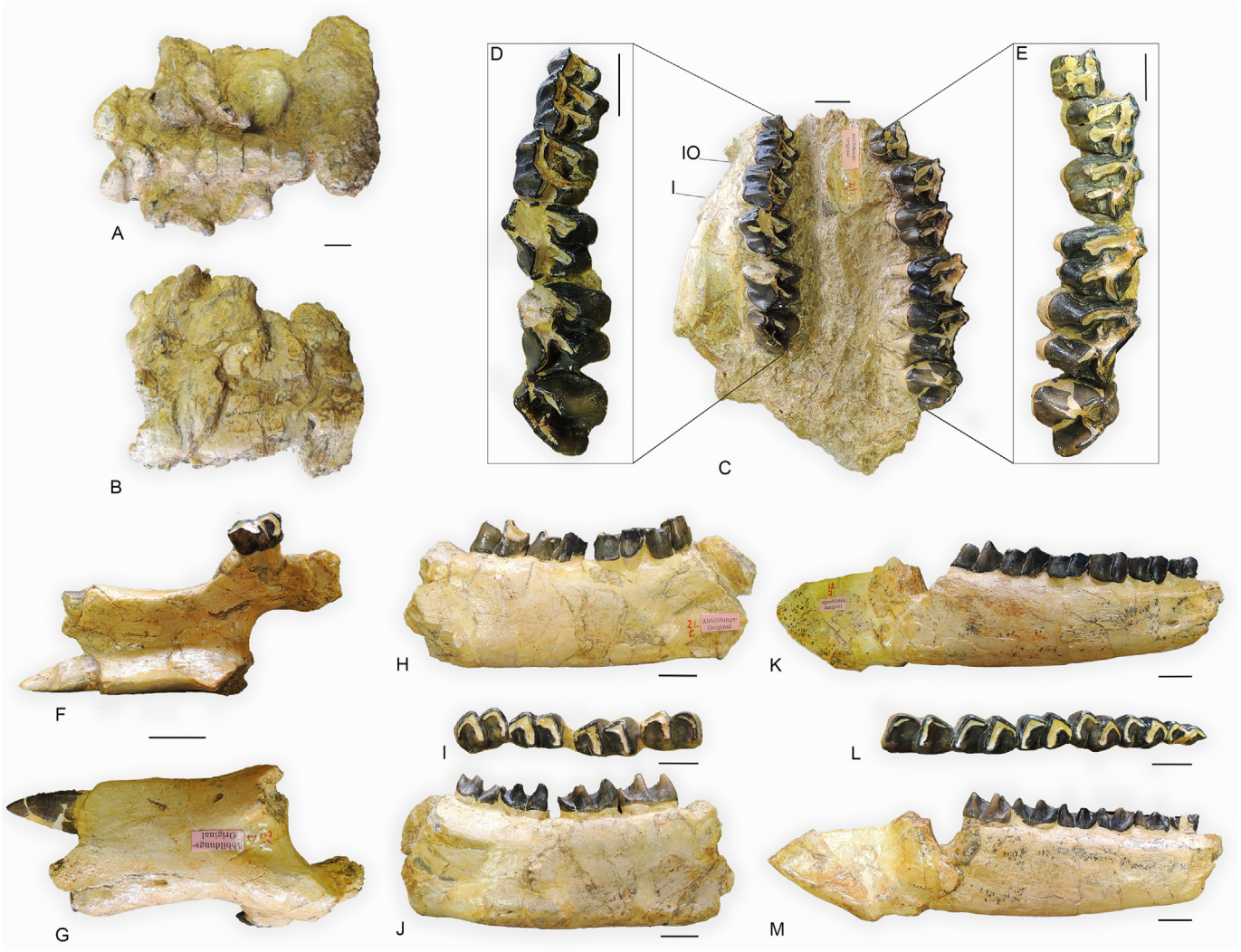

Fig. 2. Cranial remains of *Parvorhinus steinheimensis* from Devínska Nová Ves (Middle Miocene, Slovakia), NHMW 21C. (A, B) Basicranium, ventral and dorsal views. (C) Fragment of the palate with the upper cheek teeth, occlusal view. (D) Right upper cheek tooth of the palate, occlusal view. (E) Left upper cheek tooth of the palate, occlusal view. (F, G) Symphyseal portion of the mandible, dorsal and ventral views. (H–J) Right portion of the mandible, lingual, occlusal, and labial views. (K–M) Left portion of the mandible, labial, occlusal, and lingual views. Scale bar = 2 cm. IO = infraorbital foramen; I = anterior border of the orbit.

are long. P2 has a slightly convex external profile of the ectoloph, a protoloph not joined with the ectoloph, a transverse metaloph, a protocone large as the hypocone, and a small postfossette. P3 and P4 are similar in morphology; both has a constricted protoloph, protocone and hypocone weakly joined lingually, a small crochet, and a narrow postfossette. M1 and M2 has a prominent paracone fold and a concave posterior part of the ectoloph. The protocone is constricted, forming a wide antecrochet on the median valley. The hypocone is posterior to the metacone. M3 has a triangular shape; the parastyle is long, the parastyle groove is deep and the paracone fold is prominent. A simple crochet is present (Fig. 2C–E).

4.3. Mandible

Three portions of the same mandible are preserved (Fig. 2F–M). The incisor corpus (Fig. 2F, G) is rectangular in dorsal view and bears two well-developed i2s. The symphysis is nearly horizontal and massive; its posterior margin lies in front of p2. In lateral view, the foramen mentale is above p2 and the ventral border of the ramus is straight. In medial view, the lingual groove is absent.

4.4. Lower teeth

The i2s (Fig. 2F, G) have a tusk-like shape and are parallelly oriented on the incisor corpus. The lower cheek teeth (Fig. 2H–M) display a well-developed external groove that reaches the neck. The trigonid is angular and forms an acute dihedron with the talonid. Metaconid and entoconid are respectively joined with the metalophid and hypolophid. The lingual valleys are V-shaped in lingual view, lingual and labial cingula are absent, and a mesial cingulum occurs on all the teeth. On p2, the paralophid is lingually curved, the paraconid is developed and the posterior valley

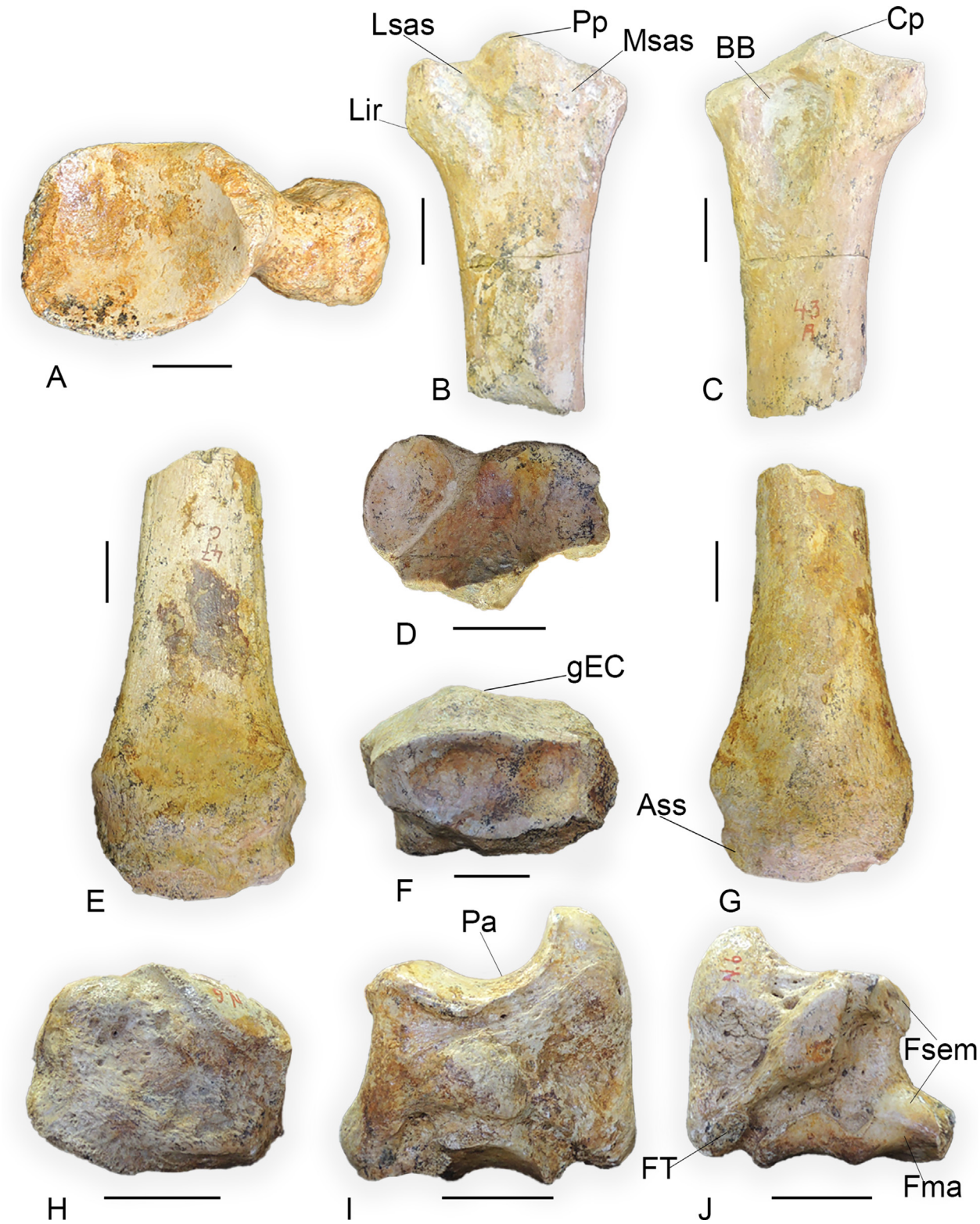

Fig. 3. Postcranial remains of *Parvorhinus steinheimensis* from Devínska Nová Ves (Middle Miocene, Slovakia). (A) Scapula distal portion (NHMW 7), articular face view. (B–D) Proximal epiphysis of radius (NHMW 43A), posterior, anterior, and proximal views. (E–G) Distal epiphysis of radius (NHMW 42A), anterior, distal articular face, and posterior views. (H) Unciform (NHMW N6), anterior view. (I, J) Scaphoid (NHMW N6), medial and lateral views. Scale bar = 2 cm. Ass = articular surface for scaphoid; BB = insertion of the biceps brachial; Cp = coracoid process; FMa = facet for magnum; Fsem = facet for semilunar; FT = facet for trapezoid; gEC = gutter for the carpal extensor; Lir = lateral insertion relief; Lsas = lateral synovial articular surface; Msas = medial synovial articular surface; Pa = proximal articulation; Pp = palmar process.

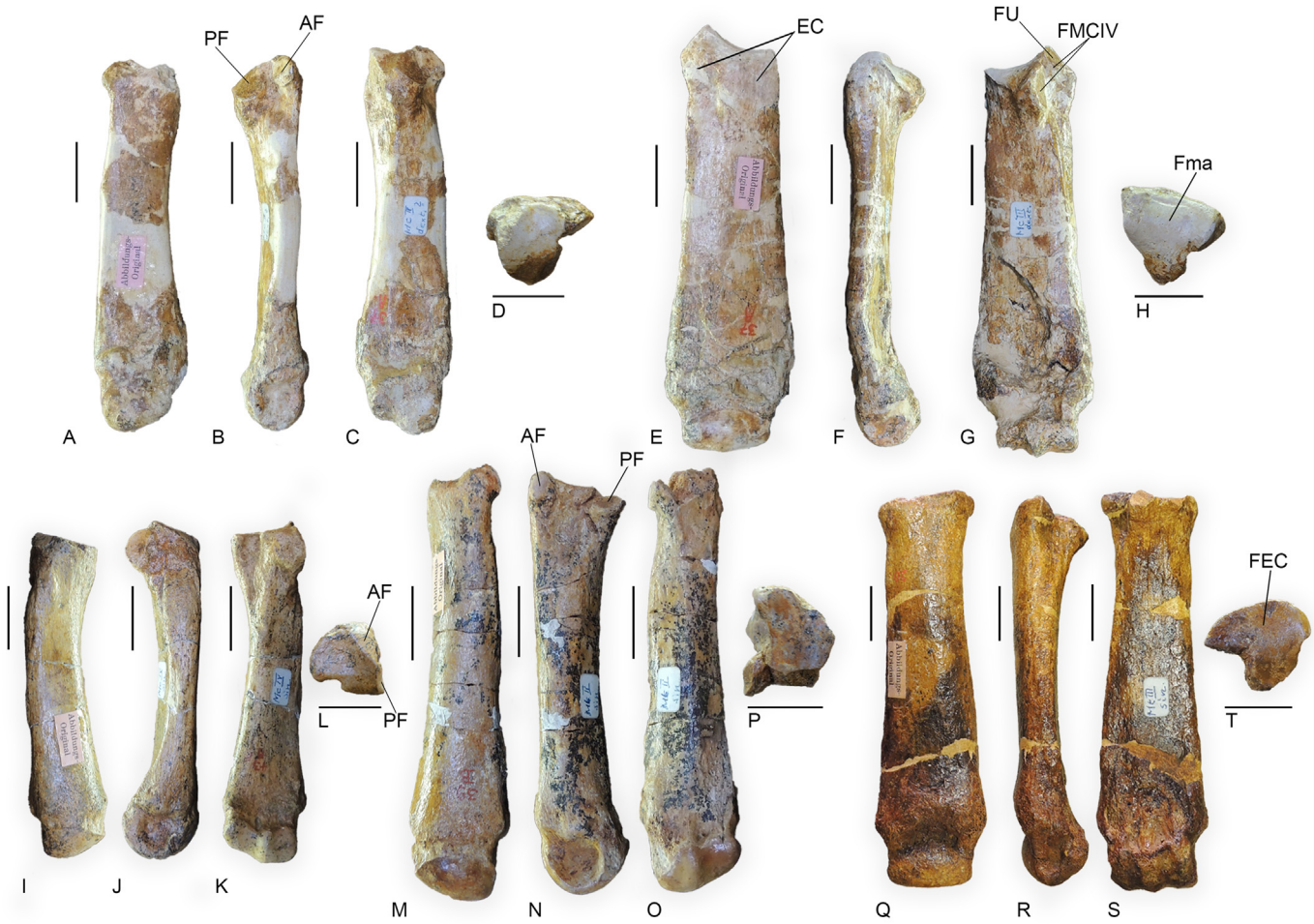

Fig. 4. Postcranial remains of *Parvorhinus steinheimensis* from Devínska Nová Ves (Middle Miocene, Slovakia). (A–D) MCII (NHMW 37A), anterior, medial, posterior, and proximal articular face views. (E–H) MCIII (NHMW 37A), anterior, medial, posterior, and proximal articular face views. (I–L) MCIV (NHMW 37A), anterior, medial, posterior, and proximal articular face views. (M–P) MTII (NHMW 39B), anterior, medial, posterior, and proximal articular face views. (Q–T) MTIII (NHMW L3), anterior, medial, posterior, and proximal articular face views. Scale bar = 2 cm. AF = anterior medial facet; EC = insertion for the extensor carpalis; FEC = facet for ectocuneiform; Fma = facet for magnum; FMCIV = facet for MCIV; FU = facet for ulna; PF = posterior medial facet.

is lingually opened. An anterior valley is also present on p2. On the molars, the hypolophid is relatively transverse, the entoconid lacks a lingual groove and the paralophid is long and reaches the lingual border of the crown.

4.5. Postcranial remains

4.5.1. Scapula

Only a distal portion of the scapula is preserved (Fig. 3A). In medial view, the inferior glenoid tubercle is small and rounded, the supraglenoid tubercle is present and the coracoid process is weak. In articular face view, the glenoid cavity is oval in shape.

4.5.2. Radius

On the posterior-proximal face of the bone (Fig. 3B), the ulna-facets are separated. On the proximal-anterior side of the bone (Fig. 3C), the insertion of the biceps brachial is shallow and the lateral tuberosity is faint. In proximal view (Fig. 3D), the anterior border of the proximal articulation is M-shaped; the lateral facet is squared and well-developed and its posterior border is rather straight. The angle between the posterior borders of the medial and lateral facets is strongly obtuse. The medial border of the proximal articulation, in anterior view, extends medially. A badly preserved distal epiphysis is present in the collection (Fig. 3E–G). On distal face view (Fig. 3F), the gutter for the carpal extensor is deep and wide, the second distal articulation for the ulna is absent and the posterior expansion of the scaphoid-facet is low (Fig. 3G).

4.5.3. Unciform

Only the anterior face of the bone is preserved (Fig. 3H). In anterior view, the anterior face is squared, and the proximal articular surface for the pyramidal is partially visible. In proximal face view, the facet for the pyramidal and that for the MCV are separated; further, the posterior expansion of the pyramidal facet is absent.

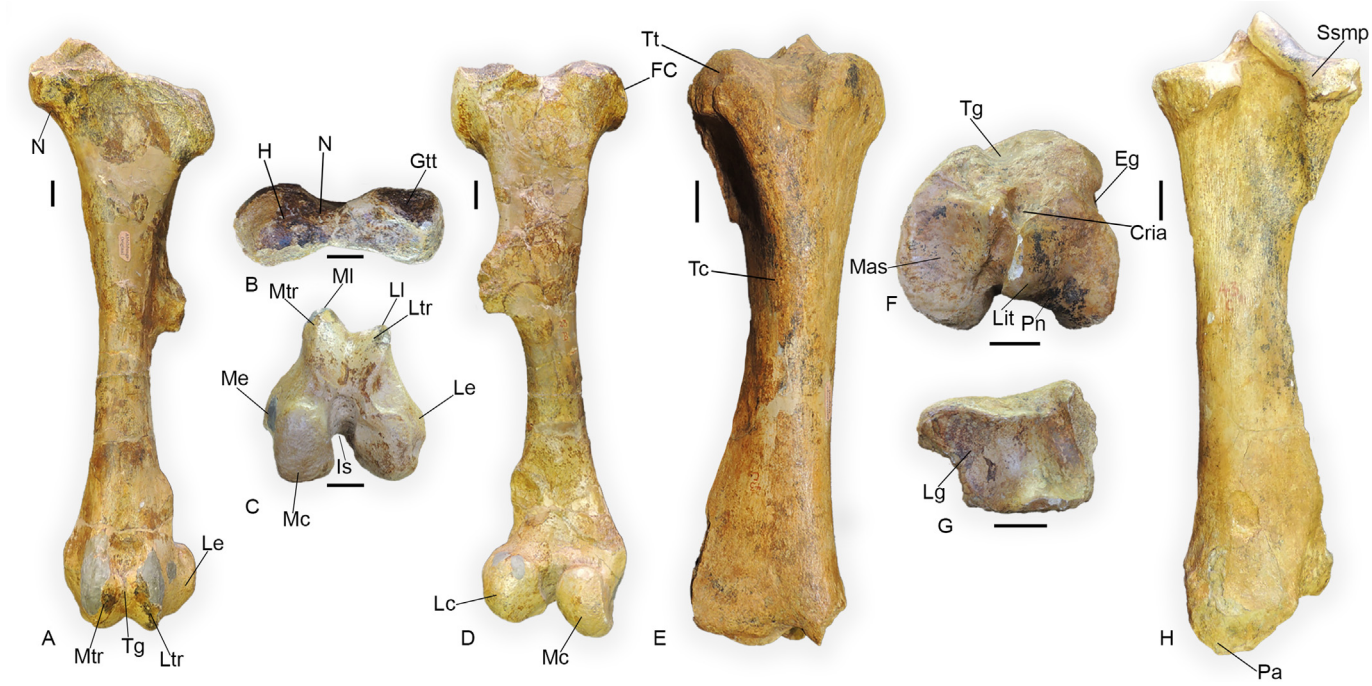

Fig. 5. Postcranial remains of *Parvorhinus steinheimensis* from Devínska Nová Ves (Middle Miocene, Slovakia), NHMW 23B. (A–D) Femur, anterior, proximal, distal, and posterior views. (E–H) Tibia, anterior, proximal, distal, and posterior views. Scale bar = 2 cm. Cria = cranial intercondylar area; Eg = extensor groove; FC = fovea capitis; Gtt = great trochanter top; H = head; Is = intercondylar space; Lc = lateral condyle; Le = lateral epicondyle; Lg = lateral groove; Lit = lateral intercondylar tubercle; Ll = lateral lip of the patellar trochlea; Ltr = lateral trochanter ridge; Mas = medial articular surface; Mc = medial condyle; Me = medial epicondyle; Ml = medial lip of the patellar trochlea; Mtr = medial trochanter ridge; Pa = posterior apophysis; Pn = popliteal notch; N = neck; Ssmp = sliding surface for muscle popliteus; Tc = interosseous crest; Tg = tuberosity groove; Tt = tibial tuberosity.

4.5.4. *Scaphoid*

In medial view (Fig. 3I), the anterior border is straight, and the proximal articulation is concave. In proximal view, the proximal articulation has a triangular outline, transversally wider on its posterior portion. In lateral view (Fig. 3J), the anterior distal articular facet for the semilunar is separated from the other distal facets by a marked groove.

4.5.5. *MCII*

The bone (Fig. 4A–D) is strongly damaged and anteriorposteriorly compressed. The proximal articular surface is longer than wide, with a rounded outline. In proximal view, the anterior facet for MCIII is visible and it is clearly not connected with the proximal articulation. In lateral view, the two facets for MCIII are distinct, have a rounded outline and the posterior facet is larger than the anterior one.

4.5.6. *MCIII*

In anterior view (Fig. 4E), the proximal outline is concave; the diaphysis is distally widening and the intermediate relief on the distal articulation is very low and shallow. The proximal border of the distal articulation is convex. The articular facets on the lateral-proximal side are large and separated by a marked groove. The anterior facet is higher than the posterior one and narrower on its distal portion. It is also divided in two facets, one for MCIV and the other for the uncinate, by a shallow saddle. In proximal view (Fig. 4H), the anterior border of the epiphysis is straight; the facet for the uncinate is partially visible. The proximal facet is anteriorly less developed than the proximal epiphysis.

4.5.7. *MCIV*

The bone (Fig. 4I–L) is well preserved. In anterior view (Fig. 4I), the lateral face of the diaphysis is regularly concave, and the distal articulation is strongly asymmetric. The proximal articular facet, in proximal view, has a triangular outline. In the same view, the two medial articular facets for MCIII are visible. The anterior one is squared, longer than high, whilst the posterior one is reniform (MCIV left) or circular (MCIV right).

4.5.8. *Femur*

The femur is relatively well-preserved (Fig. 5A–D). In anterior view, the femur head is partially damaged, but it shows a hemispheric shape and it is higher than the great trochanter. The fovea capitis is low and wide, and the third trochanter is developed and located on the mid-proximal portion of the diaphysis. The medial lip of the distal patellar trochlea is higher and more developed than the lateral one. In distal face view, the patellar trochlea is strongly asymmetric, and it is distally stopped by a wide intercondylar fossa. The posterior medial condyle is more developed

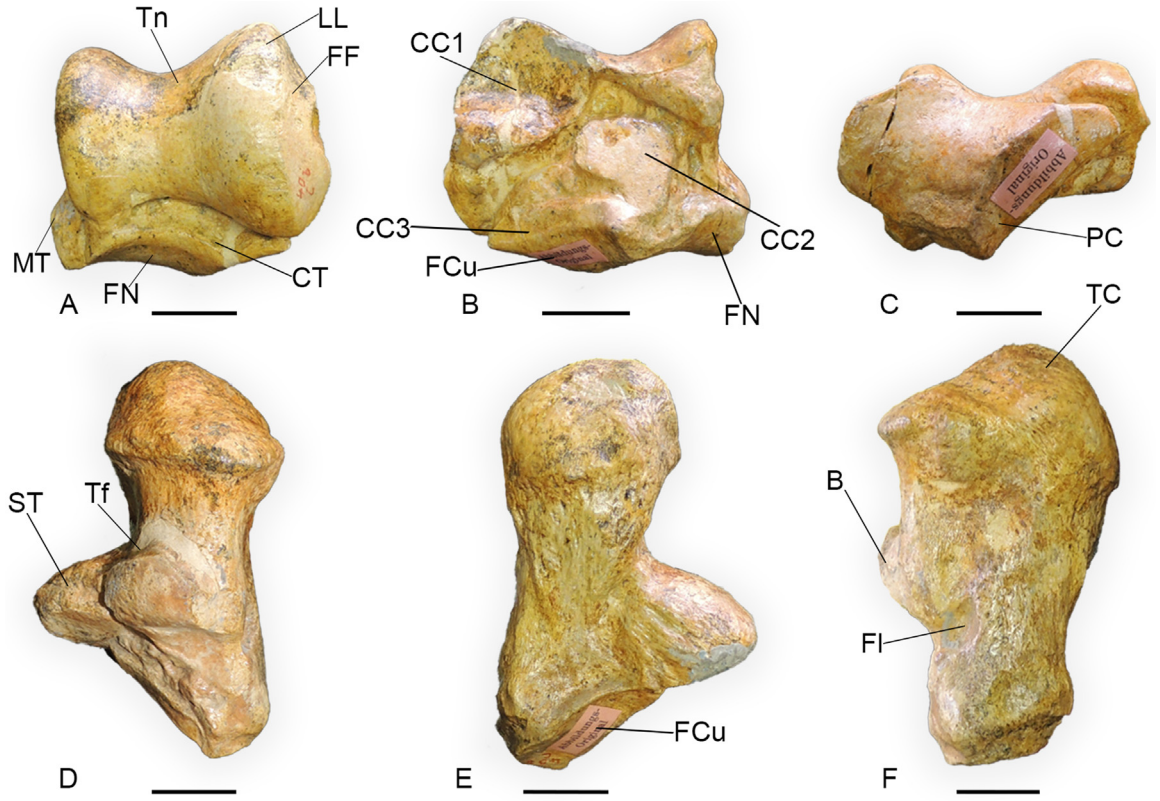

Fig. 6. Postcranial remains of *Parvorhinus steinheimensis* from Devínska Nová Ves (Middle Miocene, Slovakia), NHMW 40C. (A–C) Astragalus, anterior, posterior, and distal views. (D–F) Calcaneus, anterior, posterior, and lateral views. Scale bar = 2 cm. B = beak; CC1 = facet 1 for calcaneus; CC2 = facet 2 for calcaneus; CC3 = facet 3 for calcaneus; CT = collum tali; FCu = facet for cuboid; FF = facet for fibula; FI = insertion for the fibularis longus; FN = facet for navicular; LL = lateral lip; MT = medial tubercle; PC = posterior stop on the cuboid facet; ST = sustentaculum talii; TC = tuber calcanei; Tf = facet for the tibia; Tn = trochlea notch.

and squared than the lateral one. The medial and lateral distal tuberosities are prominent.

4.5.9. *Tibia*

The tibia (Fig. 5E–H) is well preserved. In distal view (Fig. 5G), the antero-distal groove is present, and the lateral facet of the distal articulation extends antero-laterally, resulting in a concave outline of the lateral border of the distal epiphysis. In proximal view (Fig. 5F), the tibial tuberosity is massive, and the anterior tibial groove is wide and shallow. The central intercondyloid fossa is wide and the lateral and medial portions of the tibial spine are well separated. In medial view, the medio-distal gutter is shallow. In posterior-distal view (Fig. 5H), the posterior apophysis is high and rounded.

4.5.10. *Astragalus*

The ratio between the transverse diameter and the maximal height in the astragalus is between 1 and 1.2, whilst the ratio between the anterior-posterior diameter and the maximal height is less than 0.65. In anterior view (Fig. 6A), the facet for fibula is flat, and its orientation is subvertical. The collum talii is relatively high. In posterior view (Fig. 6B), the expansion of the calcaneus facet c1 is wide and low, and the calcaneus facets c2 and c3 are in contact. In distal view (Fig. 6C), the posterior stop on the cuboid facet is present and the anterior border of the navicular facet is rather concave. The angle between the trochlea and the distal articulation is slightly oblique.

4.5.11. *Calcaneus*

In anterior view (Fig. 6D), the tibia facet is present, whilst the fibula facet is absent. In proximal view, the tuber calcanei is massive. In posterior view (Fig. 6E), the sustentaculum talii is massive and it is perpendicular to the corpus of the bone. In the same view, the cuboid facet is visible. In lateral view (Fig. 6F), the tuber calcanei is antero-posteriorly more developed than the beak, and the insertion for the fibularis longus is salient.

4.5.12. *MTII*

In anterior view (Fig. 3M), the bone is long and distally widening. The proximal border of the proximal epiphysis is concave. In medial view, two proximal articular facets are present: both are subcircular and separated by a wide groove. In proximal view, the anterior border of the proximal articular facet is sigmoidal, and the surface is longer than wide. In the same view, the two medial facets are evident.

4.5.13. MTIII

The bone is long and slender (Fig. 3M–P). The distal articular surface, in anterior view, has a convex proximal border and the intermediate relief is low and smooth. In the same view, the proximal border of the proximal epiphysis is straight, and the diaphysis widens distally. In lateral view, the proximal epiphysis bears two small triangular articular surfaces. The articular facets for the MTIV are distinct; the anterior one is rectangular and placed more proximally than the posterior one. In proximal view, the anterior border of the proximal epiphysis is rather straight.

5. Comparison

5.1. Comparison with Elasmotheres

The studied material differs from Middle Miocene Elasmotheriini (e.g., *Hispanotherium*, *Procoelodonta*, *Caementodon*) by having low crown height of the cheek teeth, simpler enamel foldings on the cheek teeth, protocone weakly constricted only on the upper molars, protocone and hypocone weakly joined on the upper premolars, and smaller dimensions (cf. Heissig, 1999; Antoine, 2002).

5.2. Comparison with Aceratheriini

Aceratheriini representatives (Guérin, 1980; Heissig, 1999; Antoine et al., 2003) generally differ from the studied specimens by the presence of well-developed crochet on the molars, presence of a well-developed antecrochet on the upper cheek teeth, well-developed lingual cingulum on the upper cheek teeth, lingually flattened protocone on the upper molars, medifossette on the upper premolars, short paralophid on the lower cheek teeth, divergent i2 on the mandible, wider incisor corpus in respect to the symphyseal area. In *Alicornops simorrense*, the DP1 is present in adult specimen (e.g., MNCN47576), the antecrochet is well-developed on the upper molars, the metacone fold is weak on the upper premolars, and protocone and hypocone are normally separated on the upper premolars. In *Hoploaceratherium tetradactylum*, the metacone is faint of the upper premolars, the protocone is strongly constricted on the upper molars, the i2s are long and divergent, the paralophid is short on the lower cheek teeth, the labial cingulum is present on the lower premolars, and the general dimensions are larger than those of the studied material.

5.3. Comparison with Teleoceratina

Teleoceratina are generally characterized by the shortening of the distal limb segments (Heissig, 1999) and are larger than those of the studied material. The teeth of Middle Miocene European Teleoceratina display labial cingula on the upper molars, short paralophid on the lower teeth, labial and lingual cingula usually present on the lower teeth. In *Prosantorhinus*, the lingual cingulum is present on the upper cheek teeth, labial cingulum is often present and the protocone constriction is strong on the upper molars (Cerdeño, 1996; Antoine et al., 2018). In *Prosantorhinus germanicus* (NHMW 2008z0043/0003) the posterior border of the symphysis is at the level of the p3 talonid, the dorsal profile of the symphysis is rather flat (concave in the studied specimen), and the incisor corpus is wider than the symphyseal area.

5.4. Comparison with Rhinocerotini

Rhinocerotini are mainly documented by three genera during the Middle–early Late Miocene: *Lartetotherium*, *Gaindatherium* and *Dihoplus*.

Lartotherium, with the specie *L. sansaniense* (Heissig, 2012), closely resembles *Parvorhinus steinheimensis*, as previously underlined by Guérin (1980), and the two taxa were mainly differentiated by their relative dimensions. However, the studied material differs from *L. sansaniense* by having a posterior border of the symphysis just in front of p2, a concave posterior profile of the ectoloph, a continuous metaloph on M1, an external groove that reaches the neck on the lower teeth, an angular trigonid, and by lacking P1 and dp1/p1 in adults, labial cingula on the lower cheek teeth, and the lingual groove on the mandibular corpus. Compared with the studied specimens, *Gaindatherium browni* has a totally ventrally closed pseudomeatus, the posterior border of the symphysis located at the level of p2-p4, i2s rostrally divergent, a lingual groove on the mandibular corpus, P1 present in adults, protocone less strong than the hypocone on P2, a posterior part of the ectoloph straight on M1-M2, an external groove that vanishes before the neck, a rounded trigonid, a dp1/p1 usually present, an equal anterior and posterior heights of the scaphoid, and a salient insertion for the extensor carpalis on the metacarpals. *Dihoplus*, with *D. schleiermacheri*, has lager size in respect to the studied specimens. Further, in *Dihoplus* the crochet on P2-P4 is usually multiple, the metaloph constriction is present on the upper premolars, P1 is always present, protocone and hypocone are separated on P2-P4, antecrochet and crista are usually present on M1-M2. Other characters can be deduced from the Data Matrix.

5.5. Comparison with other specimens of Parvorhinus steinheimensis

The morphology of the upper teeth falls within the descriptions reported by Guérin (1980) for the specimens collected at Steinheim, La Grive and Can Ponsic: premolars and molars lack of lingual and labial cingula, metacone and paracone are prominent, the crochet is always present, antecrochet and protocone constriction on the premolars are always absent and the protocone constriction on the molars is weak. For the lower teeth (five specimens from La Grive), Guérin (1980) only reported V-shaped lingual valley and absence of lingual and labial cingula; features also documented in the studied material.

A few isolated lower teeth from Göriach (Austria) (NHMW 470/1963, 1980/2094) resemble the studied material in lacking lingual and labial cingula, and in having a deep external groove that reaches the neck of the tooth, V-shaped lingual valleys, an angular trigonid, a long and simple paralophid on p2, and small size. Two isolated lower molars differ from the studied material and other remains from Göriach by the presence of a protoconid fold. A fragmentary upper cheek tooth (NHMW 1980/2094) preserves only the lingual side of P3-M3. The upper molars have a constricted protocone; all the teeth display a long and continuous metaloph, a narrow postfossette, and lack the lingual cingulum. An isolated P4 (NHMW 1980/2094) shares the following feature with the studied material: a prominent paracone and metacone folds, a long parastyle and metastyle, a single and simple crochet, a long metaloph, a protoloph weakly joined with the ectoloph.

Among the material from Steinheim, a P4 (Mfn Mb.Ma 28041) only differs from the studied specimens by having a closed medifossette. The specimen from Steinheim and that from Devínska Nová Ves share the presence of metacone and paracone folds, long parastyle, constricted protoloph, hypocone and protocone weakly joined lingually at their bases, and the absence of lingual cingulum. The medifossette has been also reported on a few isolated P4s described by Guérin (1980). Another isolated P4 from the same locality (MfN Mb.Ma 28036) is morphologically similar to those from Devínska Nová Ves as well as two isolated M3s (MfN Mb.Ma 28056): they all lack lingual and labial cingula, have a single crochet, prominent paracone and metacone fold, narrow postfossette, and long parastyle.

The two proximal epiphyses of radius from La Grive (Guérin, 1980) resemble the studied material by having a lateral proximal facet almost similar in size to the medial one, the angle between the proximal facets obtuse, the medial border of the medial facet that extends medially, the insertion for the biceps brachial shallow. The magnum from Steinheim (NHMUK; Guérin, 1980, fig. 36H) has a straight proximal border of the anterior face, similarly to the specimen from Devínska Nová Ves. No other comparisons at are present possible concerning the postcranial remains.

6. Phylogenetic analysis

Nine most parsimonious trees were obtained from a cladistic analysis in PAUP. The strict consensus tree is reported in Fig. 7 (tree length = 1365 steps, consistency index = 0.273, retention index = 0.478). The topology is similar to the one obtained by other scholars in retrieving the main Rhinocerotidae clades, i.e., Aceratheriini and Rhinocerotini (all of them with a Bremer Support > 3). Within Rhinocerotini, Teoleoceratina (Bremer Support > 3) and Rhinocerotina (Bremer Support > 3) are sister taxa. The latter clade has a large polytomy that isolates the clade including the extant Asian species and their fossil relatives, and the clade, including the extant African species and the fossil Northern Eurasian species, and the three early divergent Rhinocerotina *Lartetotherium*, *Gaindatherium* and *Parvorhinus*. Within the African and Northern Eurasian clade, supported by twenty unambiguous synapomorphies, the first dichotomy isolated the Miocene *Dihoplus schleiermacheri* and the second one has a large polytomy with the latest Miocene '*Dihoplus*' *pikermiensis*, the *Pliorhinus* clade, the *Stephanorhinus* clade, the clade with the genera *Ceratotherium* and *Diceros*. However, solving the relationships among these groups is beyond the aim of this paper. Within the Indian and South-East Eurasian clade, supported by thirteen unambiguous synapomorphies, the first dichotomy isolated the *Nesorhinus* clade (supported by eight unambiguous synapomorphies), the second isolated *Rhinoceros* clade (supported by fifteen unambiguous synapomorphies), and the last dichotomy isolated the *Dicerorhinus* clade (supported by ten unambiguous synapomorphies). Contrary to recent published trees (e.g., Antoine et al., 2003; Pandolfi et al., 2021b; Uzunidis et al., 2022), the relationships among *L. sansaniense*, *G. browni* and *P. steinheimensis* are unresolved. This result could be related with the high number of convergent characters in early Rhinocerotini as well as the poor resolution given by the characters included in the matrix. The position of *Dicerorhinus* and *Rhinoceros* within the cladogram and the resulted topology, as well as the morphology and morphometry of the studied material, leads to propose that '*Dicerorhinus*' *steinheimensis* is considered in the new genus *Parvorhinus*.

7. Conclusions

Cranial and postcranial remains of *Parvorhinus steinheimensis* have never been described in details and the species was previously known only by very little data (Guérin, 1980). The systematic revision of the rhinoceros material collected at Devínska Nová Ves (Middle Miocene, Slovakia), enabled us to describe a large sample of the Steinheim' rhinoceros and to erect the new genus, *Parvorhinus*. The material assigned to it clearly differs from the other species collected from the Middle Miocene of Europe such as *Hispanotherium matritense*, *Alicornops simorrense*, *Hoploaceratherium tetradactylum*, *Brachypotherium brachypus*, and *Lartetotherium sansaniense*. The described material also differs from *Dihoplus schleiermacheri* and *Gaindatherium browni* and is morphologically and morphometrically close to other small-sized remains from Göriach, Steinheim and La Grive previously assigned as '*Dicerorhinus*' *steinheimensis*. Guérin (1982) placed the Steinheim' rhinoceros together with *L. sansaniense*, within the subfamily Dicerorhininae, and included it into the genus *Dicerorhinus*. However, the Middle Miocene small-sized rhinoceros is distantly related with the extant *Dicerorhinus* and its fossil relatives (Fig. 7). The phylogenetic analysis places *Parvorhinus steinheimensis* within Rhinocerotina and relates it to the early divergent European Rhinocerotina species such as *L. sansaniense* and *G. browni*. *Parvorhi-*

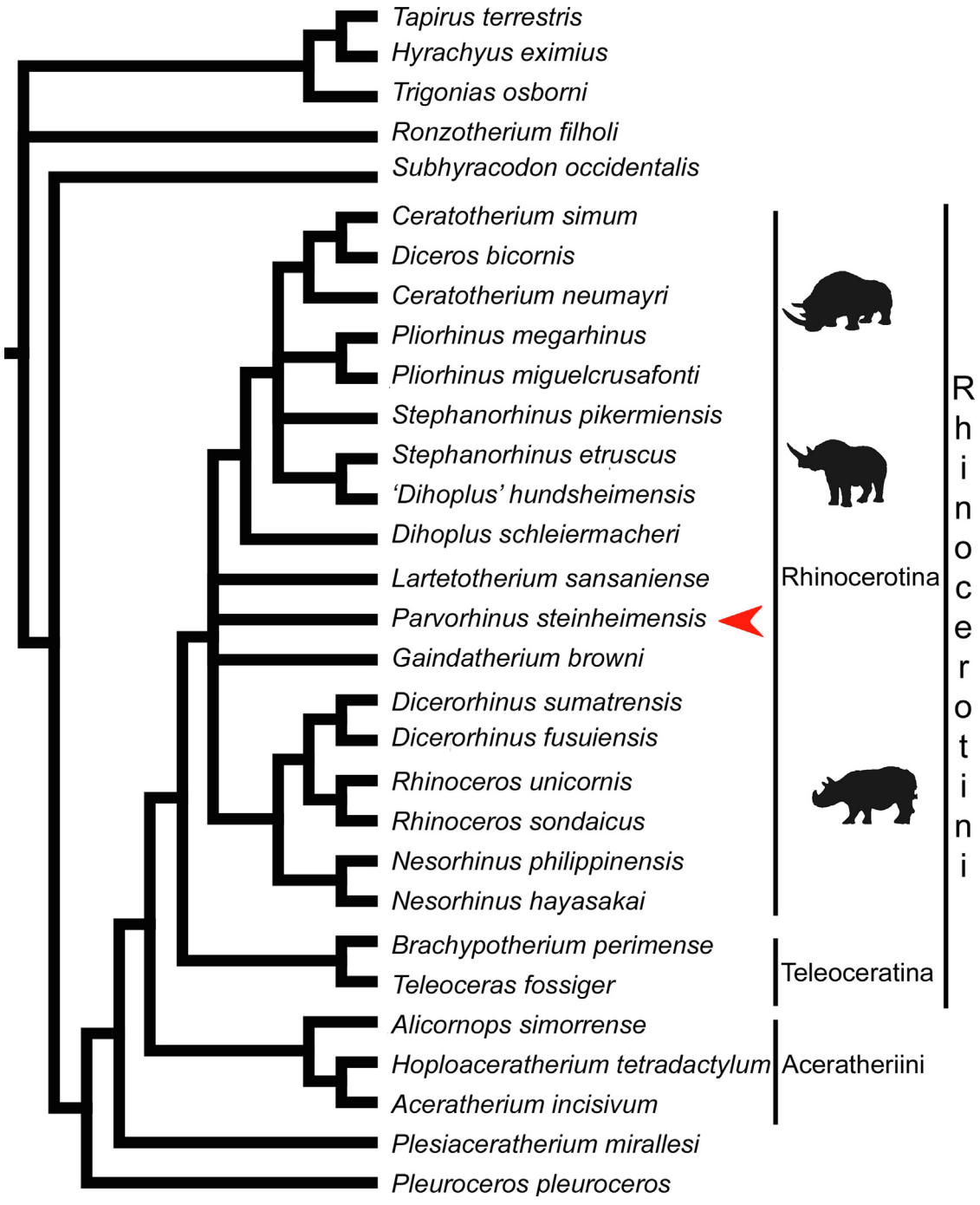

Fig. 7. Phylogenetic relationships of *Parvorhinus steinheimensis* (indicated by an arrow), within Rhinocerotini (Rhinocerotidae). The main groups discussed in the text are underlined.

nus steinheimensis is smaller and more advanced in some dental features in respect with *L. sansaniense*, such as the lack of first premolars, the absence of labial and lingual cingula and the presence of a protocone constriction on the upper molars, but it is less derived if compared with the typical Late Miocene *D. schleiermacheri*, that displays molarised upper premolars with multiple crochet, and upper molars that bear antecrochet and crista, placing it in an intermediate position within the evolutionary degree of European Miocene Rhinocerotina. Investigating the evolutionary trend within Rhinocerotina is outside the aim of this work, but it needs to be revised considering the new results here obtained and considering new characters for the cladistic analysis.

Parvorhinus steinheimensis is at present know only from MN 6 to MN 9 (Guérin, 1980; Heissig, 1999), and its fossil record is restricted to central Europe (France, Germany, Slovakia), but it cannot be excluded that the species is

underrepresented because the impossibility, till now, to compare cranial and postcranial small-sized specimens collected from other Middle Miocene localities.

Acknowledgments

We thank the Editor-in-Chief Qun Yang and reviewers (Naoto Handa and an anonymous one) for their comments and suggestions. L.P. thanks the European Community Research Infrastructure Action, EU-SYNTHESYS project AT-TAF-2550, DE-TAF-3049, GB-TAF-2825, HU-TAF-3593, HU-TAF-5477, ES-TAF-2997, IL-TAF-1324; part of this research received support from the SYNTHESYS Project http://www.synthesys.info/ which is financed by European Community Research Infrastructure Action under the FP7 'Capacities' Program. RM was granted by the PhD fellowship 2021.08458.BD by the Fundação para a Ciência e Tecnologia.

Supplementary data

Supplementary data to this article can be found online at https://doi.org/10.1016/j.palwor.2023.01.009.

References

Antoine, P.-O., 2002. Phylogénie et évolution des Elasmotheriina (Mammalia, Rhinocerotidae). Mémoires du Muséum National d'Histoire Naturelle 188, 1–359.

Antoine, P.-O., Duranthon, F., Welcomme, J.L., 2003. *Alicornops* (Mammalia, Rhinocerotidae) dans le Miocène supérieur des Collines Bugti (Balouchistan, Pakistan): implications phylogénétiques. Geodiversitas 25, 575–603.

Antoine, P.-O., Becker, D., Laurent, Y., Duranthon, F., 2018. The early Miocene teleoceratine *Prosantorhinus* aff. *douvillei* (Mammalia, Perissodactyla, Rhinocerotidae) from Béon 2, Southwestern France. Revue de Paleobiologie 37, 367–377.

Becker, D., Tissier, J., 2020. Rhinocerotidae from the early Middle Miocene locality Gračanica (Bugojno Basin, Bosnia-Herzegovina). Palaeobiodiversity and Palaeoenvironments 100, 395–412.

Boada-Saña, A., 2008. Phylogénie de *Diaceratherium* (Mammalia, Rhinocerotidae). Unpublished Master Dissertation, Université Montpellier 2, Montpellier, France, 50 pp.

Cerdeño, E., 1996. *Prosantorhinus*, the small teleoceratine rhinocerotid from the Miocene of Western Europe. Geobios, Memoire Special 29, 111–124.

Deng, T., Wang, X., Fortelius, M., Li, Q., Wang, Y., Tseng, Z.J., Takeuchi, G.T., Saylor, J.E., Säilä, L.K., Xie, G., 2011. Out of Tibet: Pliocene woolly rhino suggests high-plateau origin of ice age megaherbivores. Science 333, 1285–1288.

Gray, J.E., 1821. On the natural arrangement of vertebrose animals. London Medical Repository 15, 296–310.

Guérin, C., 1980. Les Rhinocéros (Mammalia, Perissodactyla) du Miocène terminal au Pléistocène supérieur en Europe occidentale: Comparaison avec les espèces actuelles. Documents du Laboratoire de Géologie de l'Université de Lyon 79, 1–1184.

Guérin, C., 1982. Les Rhinocerotidae (Mammalia, Perissodactyla) du Miocène terminal au Pleistoène supérieur d'Europe Occidentale comparés aux espèces actuelles: Tendances évolutives et relations phylogénétiques. Geobios, Memoire Special 15, 599–605.

Heissig, K., 1999. 16. Family Rhinocerotidae. In: Rössner, G.E., Heissig, K. (Eds.), The Miocene Land Mammals of Europe. Pfeil, Munich, pp. 175–188.

Heissig, K., 2012. Les Rhinocerotidae (Perissodactyla) de Sansan. In: Peigné, S., Sen, S. (Eds.), Mammifères de Sansan. Mémoires du Museum National d'Histoire Naturelle, Paris, pp. 317–485.

Jaeger, G.F., 1839. Über die fossilen Säugethiere, welche in Würtemberg in verschiedenen Formationen aufgefunden worden sind, nebst geognostischen Bemerkungen über diese Formationen. Carl Erhard, Stuttgart, 212 pp.

Jame, C., Tissier, J., Maridet, O., Becker, D., 2019. Early Agenian rhinocerotids from Wischberg (Canton Bern, Switzerland) and clarification of the systematics of the genus *Diaceratherium*. PeerJ 7, e7517, doi: 10.7717/peerj.7517.

Owen, R.M., 1848. Description of teeth and proportion of jaws of two extinct Anthracotherioid quadrupeds (*Hyopotamus vectianus* and *Hyopotamus bovinus*) discovered by the Marchioness of Hastings in the Eocene deposits on the NW coast of the Isle of Wight: with an attempt to develop Cuvier's idea of the classification of pachyderms by the number of their toes. Quarterly Journal of the Geological Society of London 4, 103–141.

Pandolfi, L., Calvo, R., Grossman, A., Rabinovich, R., 2021a. Rhinocerotidae from the early Miocene of the Negev (Israel) and implications for the dispersal of early Neogene rhinoceroses. Journal of Paleontology 95, 1340–1351.

Pandolfi, L., Antoine, P.-O., Bukhsianidze, M., Lordkipanidze, D., Rook, L., 2021b. Northern Eurasian rhinocerotines (Mammalia, Perissodactyla) by the Pliocene–Pleistocene transition: phylogeny and historical biogeography. Journal of Systematic Palaeontology 19, 1031–1057.

Sabol, M., Joniak, P., Bilgin, M., Bonilla-Salomòn, I., Cailleux, F., Čerňanský, A., Malíková, V., Šedivá, M., Tóth, C., 2021. Updated Miocene mammal biochronology of Slovakia. Geologica Acta 72 (5), 425–443.

Swofford, D.L., 2001. PAUP* (phylogenetic analysis using parsimony [*and other methods] version 4.0β10). Sinauer, Sunderland, MA.

Toula, F., 1884. Uber *Amphicyon*, *Hyaemoschus* und *Rhinoceros* (*Aceratherium*) von Göriach bei Turnau in Steiermark. Sitzungberichte der Kaiserlich Akademie der Wissenschaften (Mathematisch-Naturwissenschaftlichen Classe) 90 (1), 406–428.

Uzunidis, A., Antoine, P.-O., Brugal, P., 2022. A Middle Pleistocene *Coelodonta antiquitatis praecursor* (Mammalia, Perissodactyla) from Les Rameaux, SW France, and a revised phylogeny of *Coelodonta*. Quaternary Science Reviews 288, 107594.

Zapfe, H., 1949. Eine miozäne Säugetierfauna aus einer Spaltenfüllung bei Neudorf an der March (ČSR). Anzeiger der Akademie der Wissenschaften in Wien, Mathematische-naturwissenschaftliche Klasse 86, 173–181.

Zapfe, H., 1958. The skeleton of *Pliopithecus* (*Epipliopithecus*) *vindobonensis* Zapfe and Hürzeler. American Journal of Physical Anthropology 16, 441–457.

Zapfe, H., 1979. *Chalicotherium grande* (BLAINV.) Aus Der Miozänen Spaltenfüllung von Neudorf an Der March (Děvinská Nová Ves), Tschechoslowakei. Neue Denkschriften des Naturhistorischen Museums in Wien 2, 1–282.